Supplementary Material

A simple self-corrosion method constructs the Ni_3S_2@FeOOH heterostructure enables industrialized seawater oxidation

Yujie Yuan,[a,1] Ziyu Yang,[a,1] Hao Wang,[a,1] Tong Wu,[a] Xiaoyi Zhang,[a] Lin Chen,[a] Zhaohuan Wei,[b,*] Rui Wang,[c] C. Venkata Reddy,[d] Jaesool Shim[d,*], Hui Tang,[a,*]

[a] *School of Materials and Energy, University of Electronic Science and Technology of China, Chengdu 611731, Sichuan, China*

[b] *School of Physics, University of Electronic Science and Technology of China, Chengdu 611731, Sichuan, China*

[c] School of Mechanical and Electrical Engineering, Chengdu University of Technology, Chengdu, 610059, China

[d] School of Mechanical Engineering, Yeungnam University, Gyeongsan 38541, Republic of Korea

[*]Corresponding Author

DFT calculations: All the calculations were performed within the framework of the density functional theory (DFT) as implemented in the Vienna Ab initio Software Package (VASP) code within the Perdew-Burke-Ernzerhof (PBE) generalized gradient approximation and the projected augmented wave (PAW) method.[1] The cutoff energy for the plane-wave basis set was set to 450 eV. Monkhorst–Pack special k-point meshes of 3 × 3 × 1 were proposed to carry out geometry optimization and electronic structure calculation. During the geometry optimization, all atoms were allowed to relax without any constraints until the convergence thresholds of maximum force and energy were smaller than 0.01 eV/Å and 1.0×10^{-5} eV/atom, respectively.[2] A vacuum layer of 15 Å was introduced to avoid interactions between periodic images. The intermolecular van der Waals forces were corrected using the method of DFT-D3.[3] The adsorption energy (E_{ads}) of the anions is calculated by the equation: $E_{ads} = E_{total} - E_{catalyst} - E_{mol}$, in which the E_{total} represents the total energy; $E_{catalyst}$ represents the catalyst model energy; and E_{mol} represents the energy of adsorbed anions. The Gibbs free energy of each elementary step was calculated as：

$$\Delta G = \Delta E + \Delta ZPE - T\Delta S$$

where ΔE is the total energy difference between the pristine surface and adsorbing surface calculated. ΔZPE and ΔS refer to the change in zero-point energies and entropy during the reaction, respectively. The Gibbs free energy correction for enthalpy and entropy at standard condition (1 atm, 298.15K) was considered.

Figure S1. Digital photography of Ni_3S_2@FeOOH/NF with a large size.

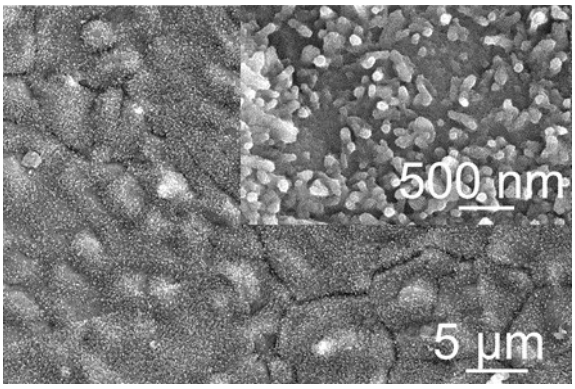

Figure S2. Low- and high-magnification SEM images of Ni_3S_2/NF.

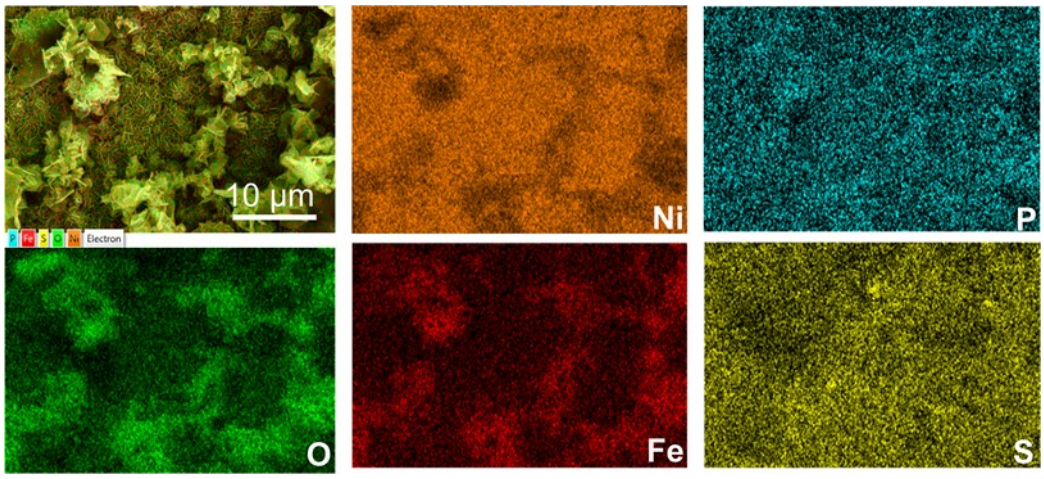

Figure S3. SEM and corresponding EDX elemental mapping images of Ni_3S_2@FeOOH/NF.

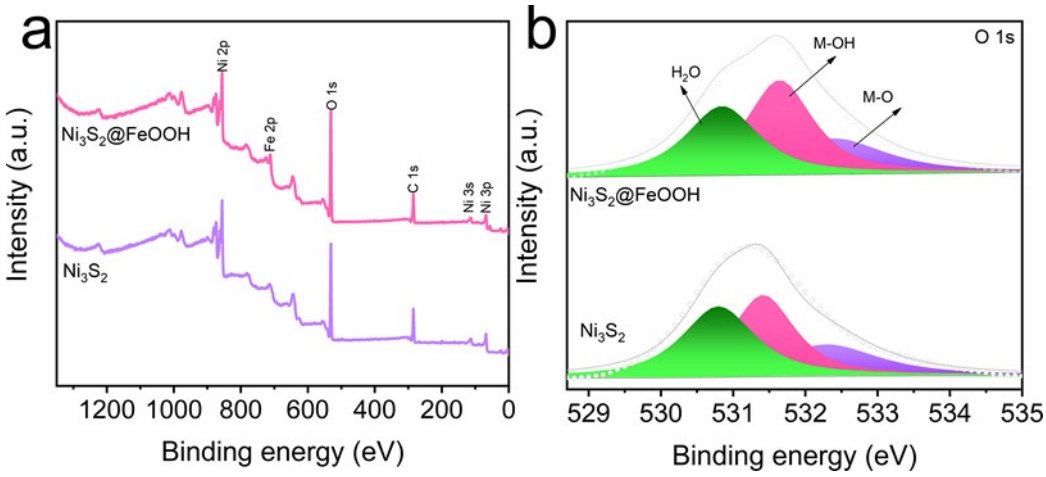

Figure S4. Survey spectrum and high-resolution XPS spectrum for Ni_3S_2/NF and Ni_3S_2@FeOOH/NF.

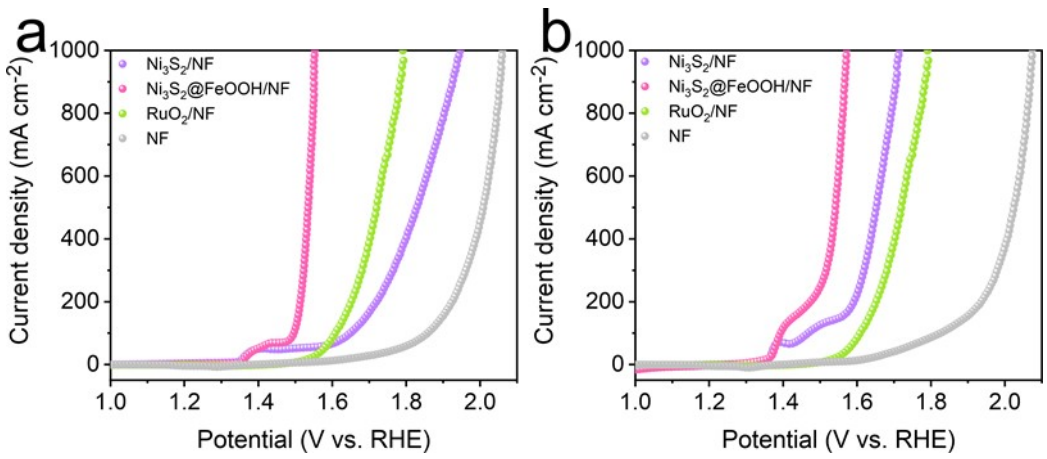

Figure S5. LSV curves of Ni_3S_2/NF and Ni_3S_2@FeOOH/NF, RuO_2/NF, and NF in 1 M KOH (with 90%iR correction). (a) 1 M KOH. (b) 1 M KOH + 0.5 M NaCl.

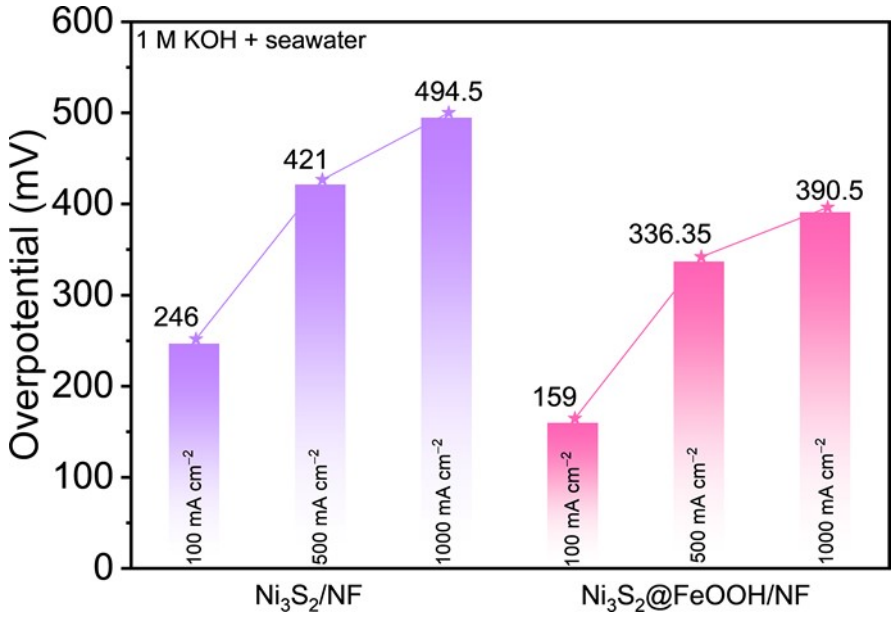

Figure S6. Comparison of the overpotential and stability of Ni_3S_2/NF and Ni_3S_2@FeOOH/NF in 1 M KOH + seawater at 1000 mA cm^{-2}.

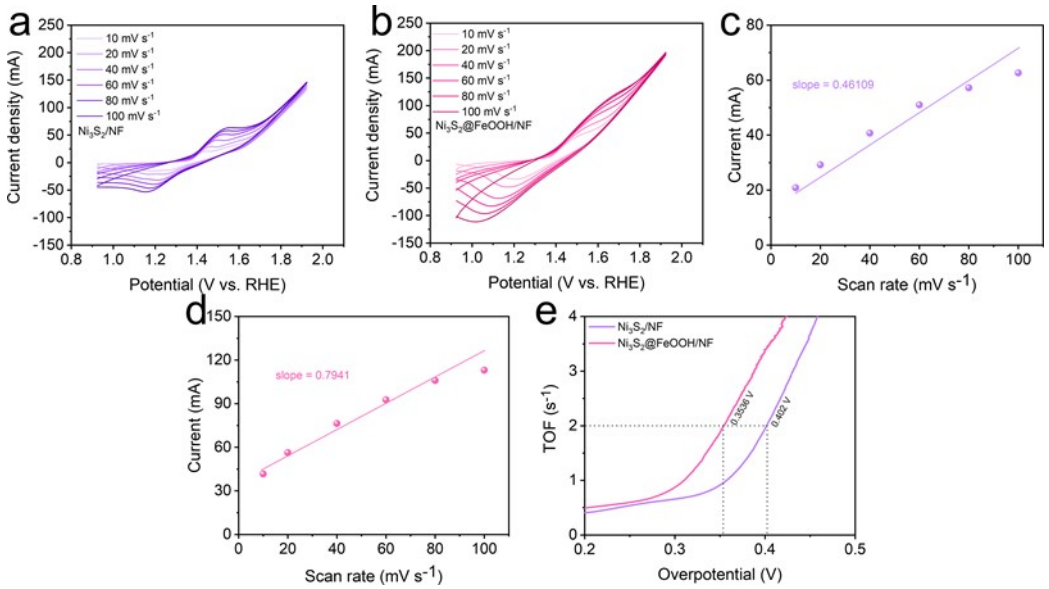

Figure S7. CV curves for (a) Ni_3S_2/NF, (b) Ni_3S_2@FeOOH/NF at different scan rates increasing from 10 to 100 mV s^{-1} in alkaline seawater. Oxidation peak current versus the scan rate plot for (c) Ni_3S_2/NF, (d) Ni_3S_2@FeOOH/NF, (e) TOF plot.

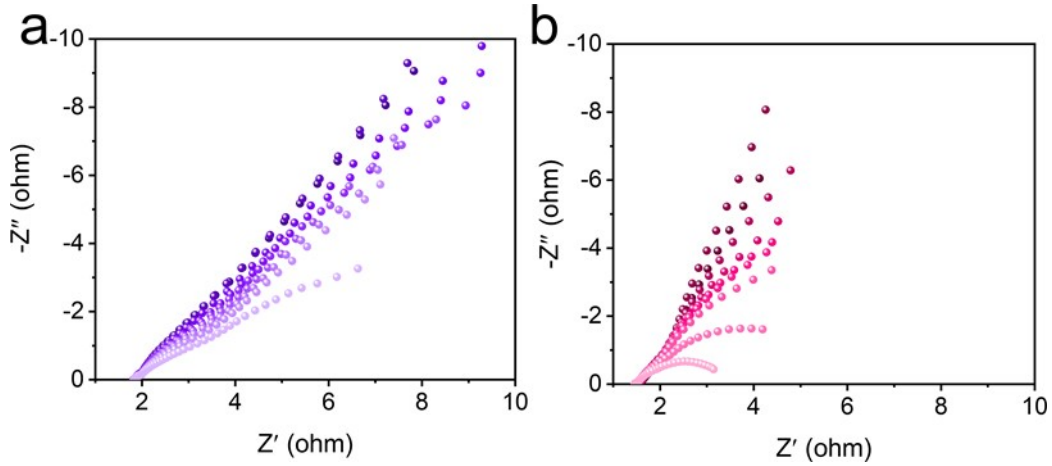

Figure S8. Bode plots corresponding to Nyquist plots for (a) Ni_3S_2/NF and (b) Ni_3S_2@FeOOH/NF.

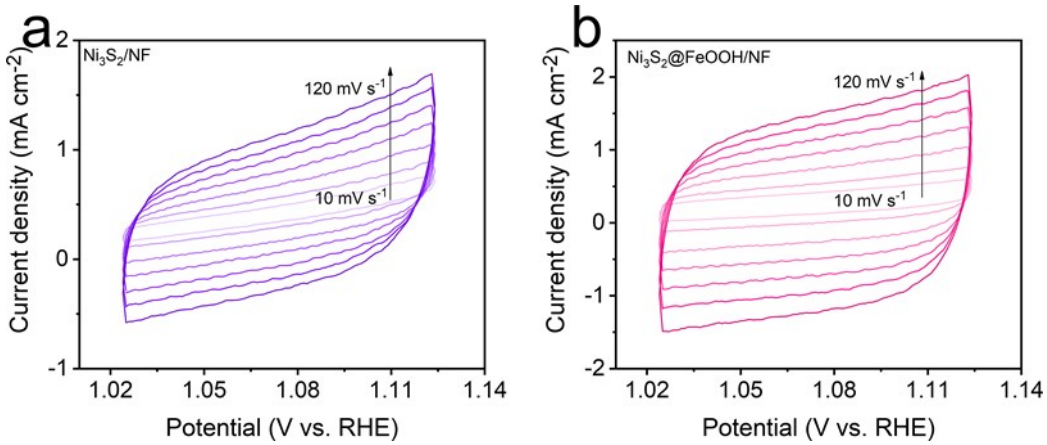

Figure S9. CV curves for (a) Ni_3S_2/NF, (b) Ni_3S_2@FeOOH/NF in the double layer region at different scan rates of 10, 20, 40, 60, 80, 100, 120, and 140 mV s^{-1} in 1 M KOH + seawater.

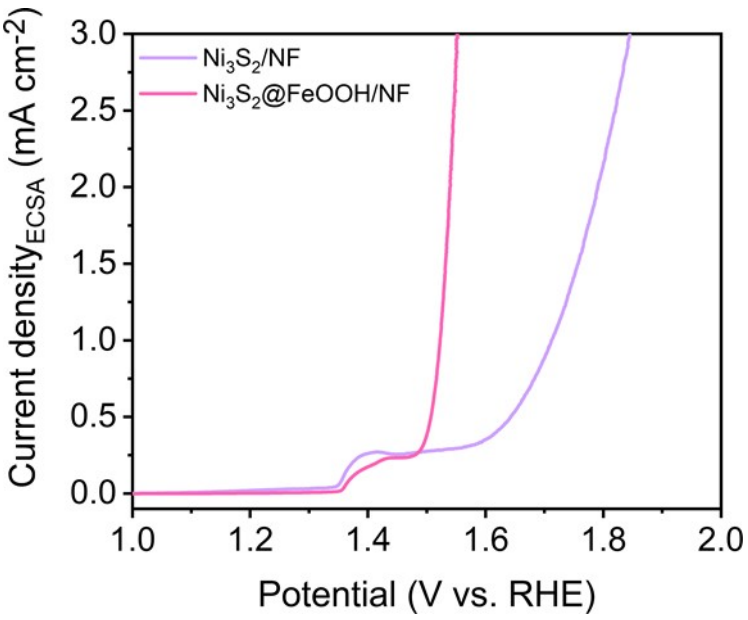

Figure S10. LSV curves normalized by electrochemical active surface area for Ni_3S_2/NF and Ni_3S_2@FeOOH/NF in 1 M KOH + seawater.

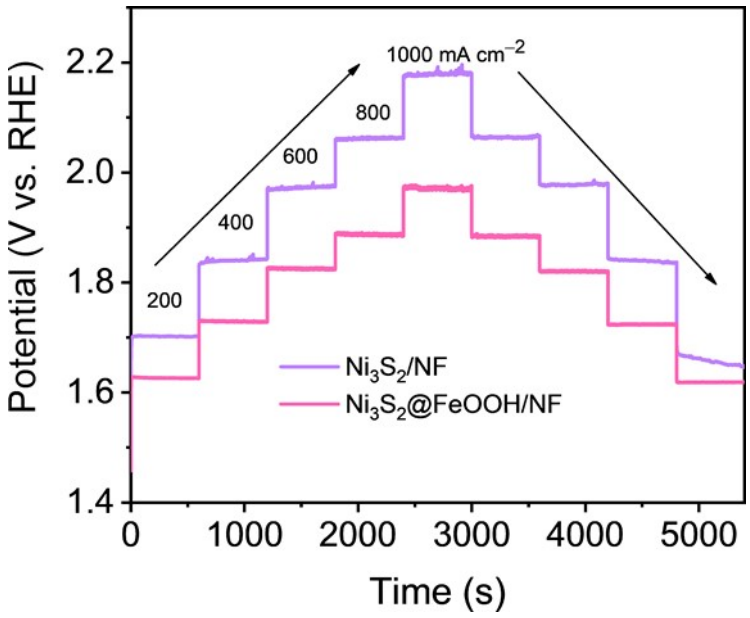

Figure S11. Multistep chronopotentiometric curves of Ni_3S_2/NF and Ni_3S_2@FeOOH/NF without iR-correction.

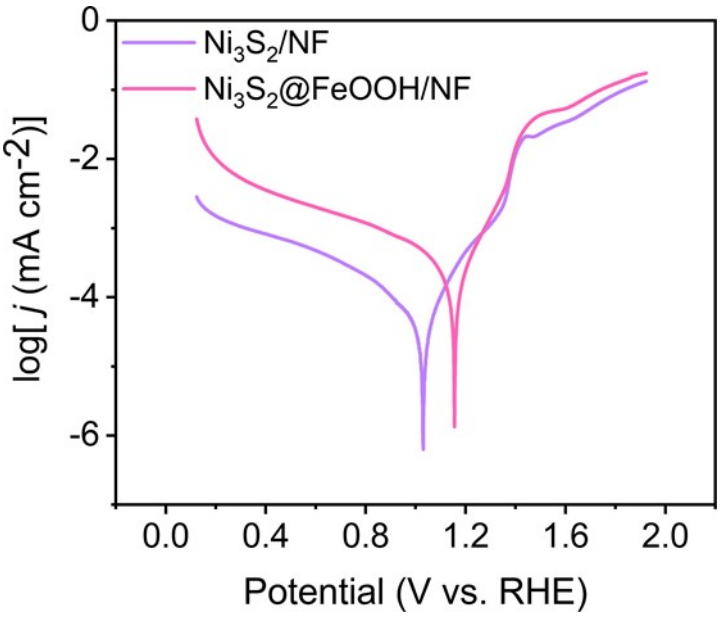

Figure S12. Corrosion polarization curves of Ni_3S_2/NF and Ni_3S_2@FeOOH/NF in 1 M KOH + seawater.

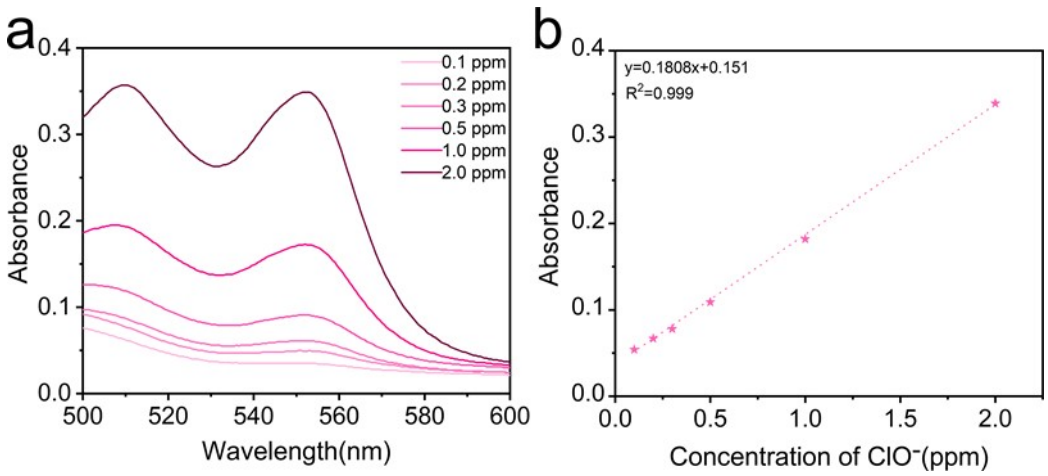

Figure S13. (a) UV-vis absorption spectra of various active chlorine concentrations and (b) the corresponding linear fit.

Determination of active chlorine: The concentration of active chlorine in the electrolyte was determined based on the DPD method using a UV-vis spectrophotometer. Firstly, the 100 μL of stability-tested electrolyte was successively mixed with 50 μL of H_2SO_4 (1.0 M), 50 μL of NaOH (2.0 M), and 4.8 mL of deionized water. Then, 250 μL of DPD reagent and 250 μL of PBS (pH = 6.5) were added to the above solution. After two minutes of color development away from light, the color of the solution turns transparent pink. The absorbance at 550 nm was determined by UV-vis absorption spectrometry, and the concentrations of different active chlorine were analyzed [4-5].

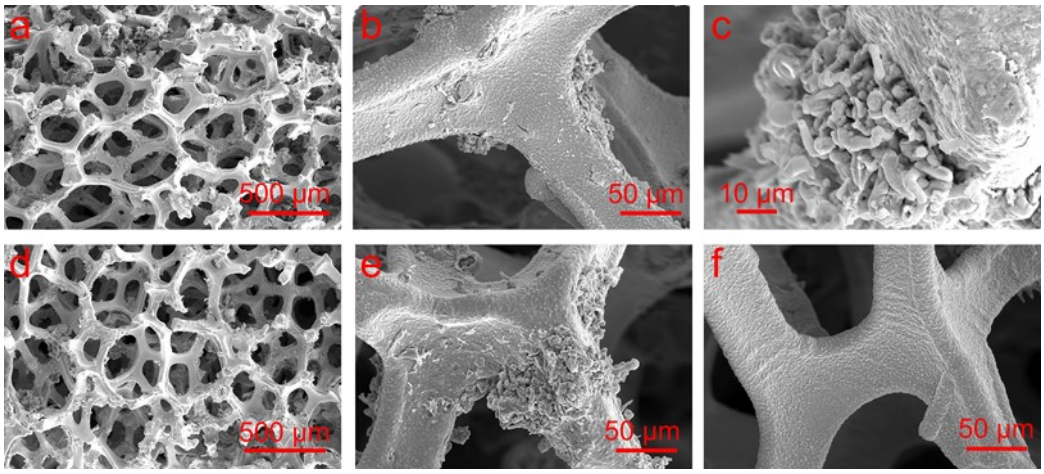

Figure S14. SEM images of Ni_3S_2@FeOOH/NF after stability at 1000 mA cm^{-2} (a-c) and 2000 mA cm^{-2} (d-f) in 1 M KOH + seawater.

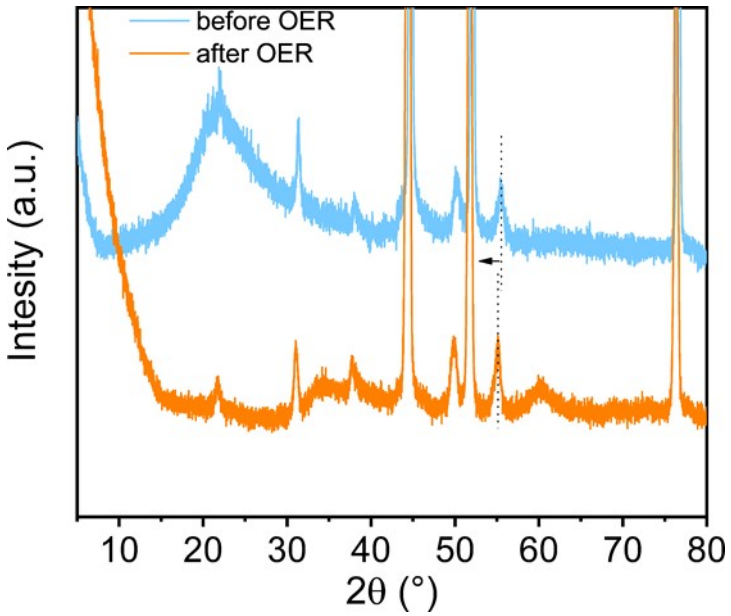

Figure S15. XRD patterns of Ni_3S_2@FeOOH/NF before and after the stability test in 1 M KOH + seawater.

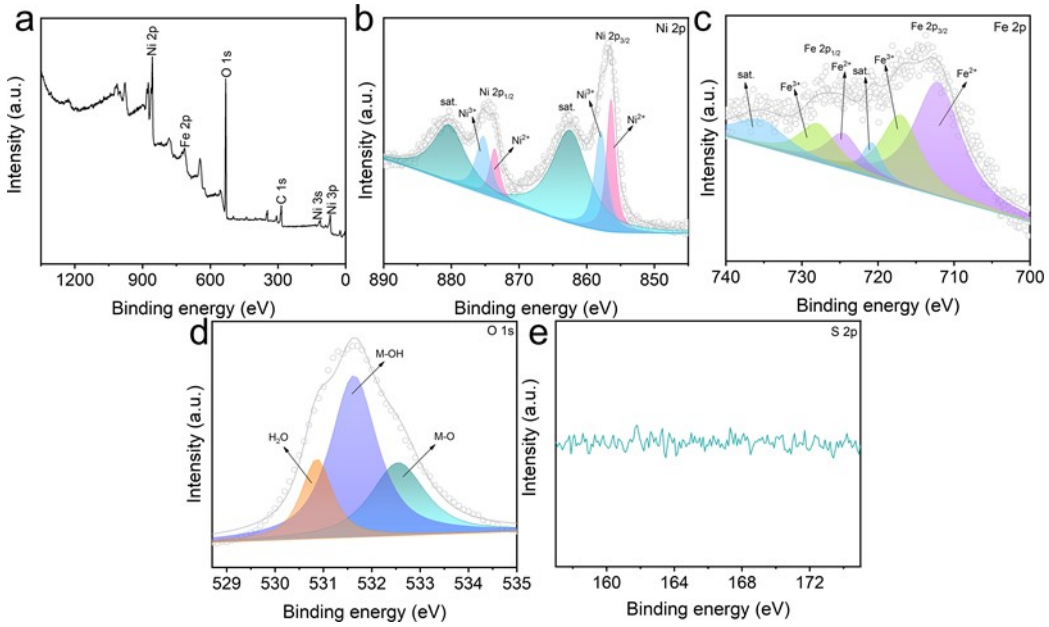

Figure S16. (a) Survey spectrum of XPS for Ni_3S_2@FeOOH/NF after the stability test. XPS spectra of Ni_3S_2@FeOOH/NF in the (b) Ni 2p, (c) Fe 2p, (d) O 1s, and (e) S 2p regions after the stability test.

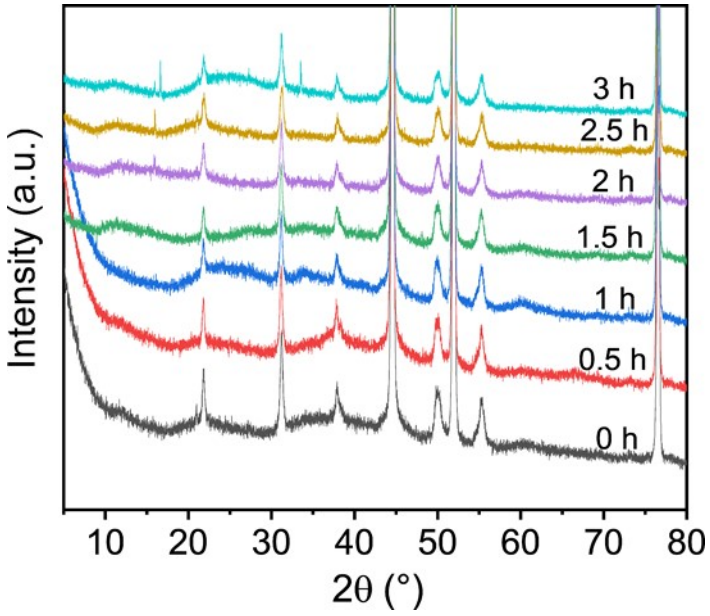

Figure S17. In situ XRD spectra of Ni_3S_2@FeOOH/NF.

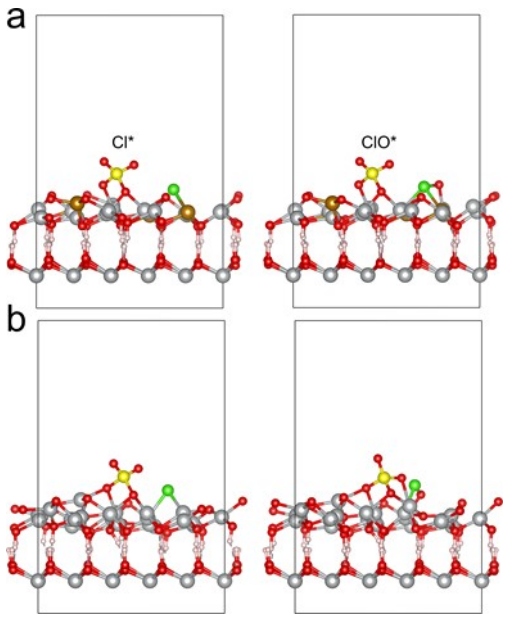

Figure S18. Possible ClOR pathways of (a) SO_4^{2-}-NiFeOOH and (b) SO_4^{2-}-NiOOH.

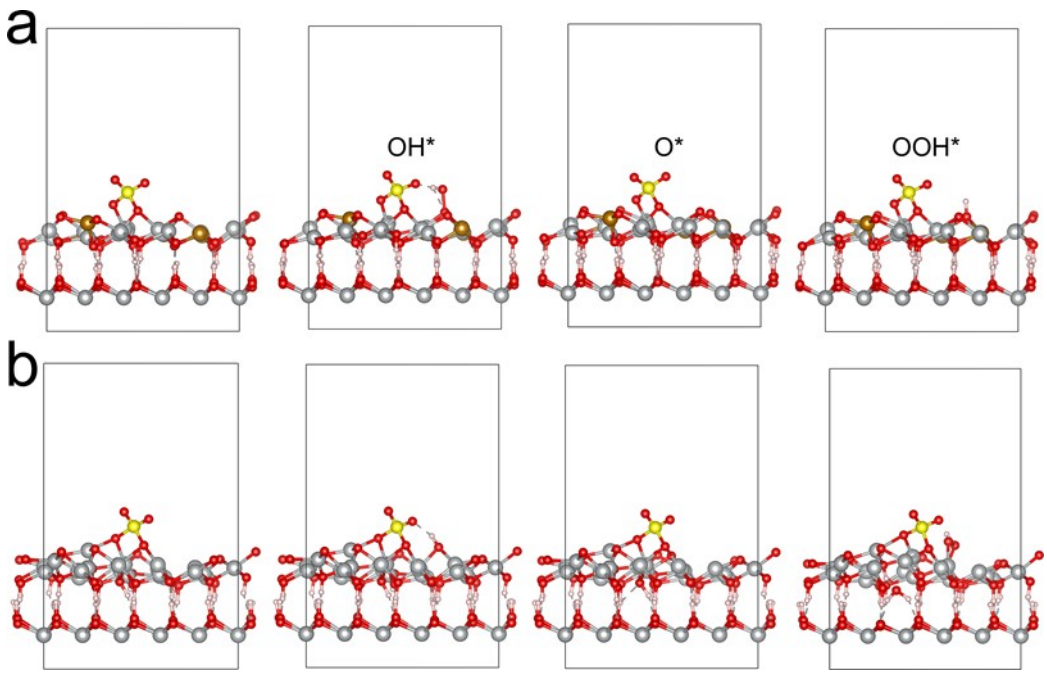

Figure S19. Possible AEM-based pathways of (a) SO_4^{2-}-NiFeOOH and (b) SO_4^{2-}-NiOOH.

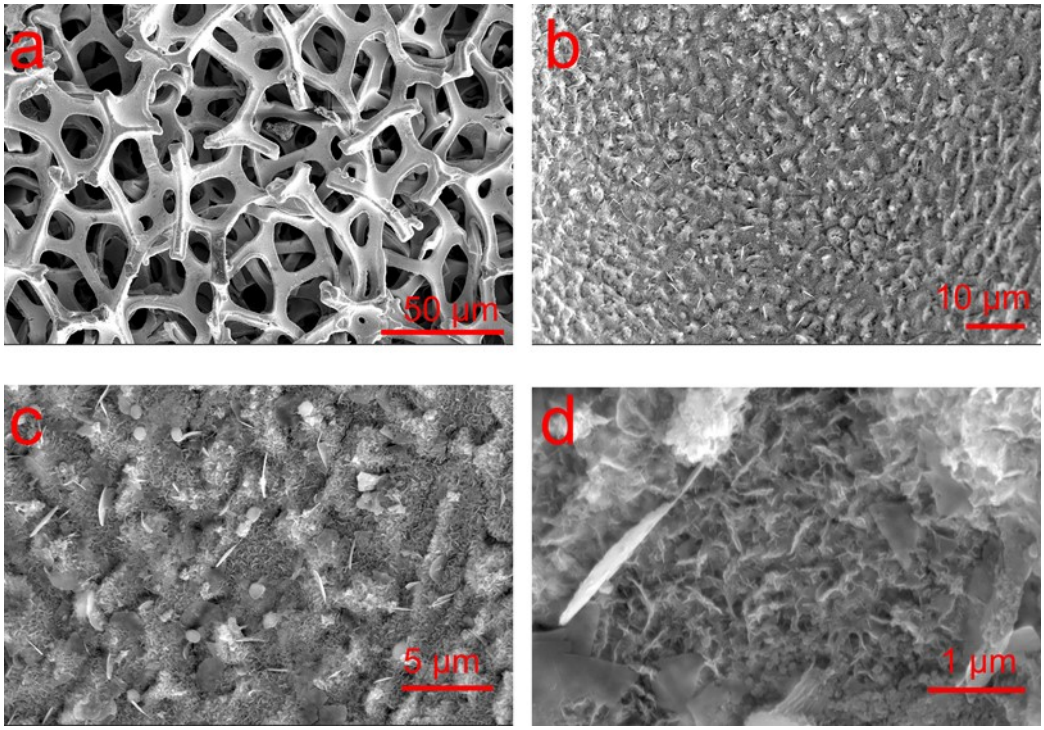

Figure S20. SEM image of Ni_3S_2@FeOOH/NF after long-term flow cell operation.

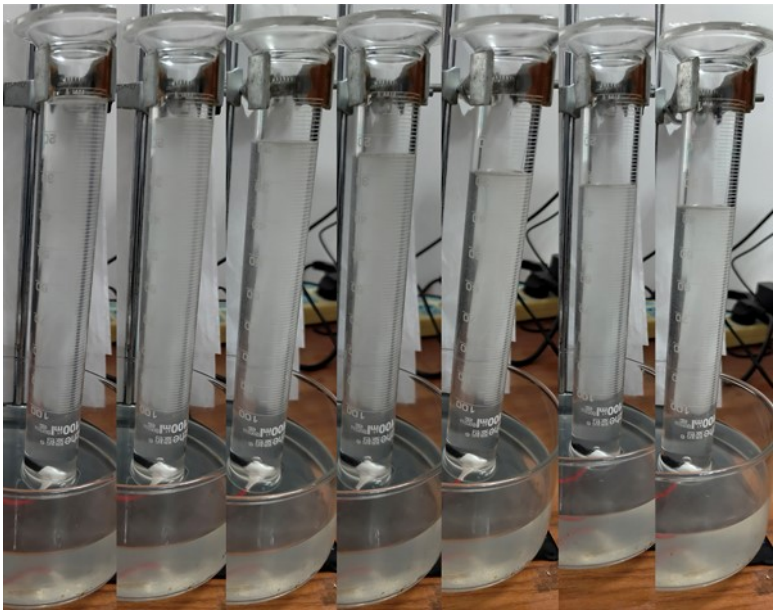

Figure S21. Collection of oxygen evolved from seawater oxidation at the *j* of 1000 mA cm^{-2} by water drainage method.

Table. S1 Comparison of OER catalytic activity for Ni_3S_2@FeOOH/NF with recently reported catalysts in alkaline seawater.

Catalyst	*j*@time@η	electrolyte	Refrence
NiFeO-CeO_2/NF	1000 mA cm^{-2}@200 h@408 mV	1 M KOH + seawater	ACS Nano. 2023, 17, 16008−16019.
FeMoOOH	1500 mA cm^{-2}@1000 h	1 M KOH + seawater	Energy Environ. Sci. 2025, 18, 1952–1962.
Ni(OH)$_2$-$P_3O_{10}^{5-}$	1400 mA cm^{-2}@240 h	1 M KOH + seawater	Adv. Energy Mater. 2025, 15, 2402883.
F-NiFe-LDH	1000 mA cm^{-2}@1000 h	1 M KOH + seawater	Adv. Funct. Mater. 2025, 2423965.
FeCoNiMoV oxide	1000 mA cm^{-2}@100 h	1 M KOH + seawater	Chemical Engineering Journal. 2024, 495, 153408.
MoNiP	1000 mA cm^{-2}@1500 h	1 M KOH + 0.5 M NaCl	Adv. Energy Mater. 2025, 15, 2403009.
NFCVM-5	1000 mA cm^{-2}@500 h	1 M KOH + seawater	Small. 2024, 20, 2402720.
MoO_3@CoO/CC	600 mA cm^{-2}@1000 h	1 M KOH + seawater	Nature Communications. 2024, 15, 2481.
CoFePBA/Co_2P	1000 mA cm^{-2}@1000 h	20 wt% NaOH + seawater	Angew. Chem. Int. Ed. 2023, 62, e202309882.
CoFeAl-LDH	1000 mA cm^{-2}@500 h	1 M KOH + seawater	Nature Communications. 2024, 15, 4712.
NiFe-LDH-CO_3^{2-}	500、1000 mA cm^{-2}@1000 h	1 M KOH + 0.5 M NaCl + 1 M Na_2CO_3	Adv. Energy Mater. 2024, 14, 2400053.
Ir-CoFe-LDH	400-800 mA cm^{-2}@1000 h	6 M NaOH+2.8 M NaCl	Nature Communications. 2024, 15, 1973.
$Ru_{0.1}$-NiFeOOH-PO_4^{3-}	500 mA cm^{-2}@1000 h	1 M KOH + seawater	EES Catal. 2024, 2, 1092–1099.
NiFe-CuCo LDH	500 mA cm^{-2}@500 h	6 M KOH + seawater	PNAS. 2022, 119, e2202382119.
$NiCoP_v$@NF	500 mA cm^{-2}@110 h	1 M KOH + seawater	Adv. Energy Mater. 2024, 14, 2400975.
Ru-Ni_2P/Fe_2P	500 mA cm^{-2}@100 h	1 M KOH + seawater	Adv. Funct. Mater. 2024, 34, 2400734.
Fe_3Se_4-$NiSe_2$@Mxene	500 mA cm^{-2}@140 h@300 mV	1 M KOH + seawater	Adv. Funct. Mater. 2025, 2424718.
(Ni,Fe)OOH@Ni_xP	500 mA cm^{-2}@100 h@318 mV	1 M KOH + seawater	Applied Catalysis B: Environmental. 2023, 336, 122926.
SO_4^{2-}/CoFe LDH	500 mA cm^{-2}@1000 h	1 M KOH + seawater	Adv. Funct. Mater.

			2025, 2419871.
RuMoNi	500 mA cm^{-2}@3000 h	1 M KOH + seawater	Nature Communications. 2023, 14, 3607.
Os-Ni_4Mo/MoO_2	500 mA cm^{-}2@2500 h@336 mV	1 M KOH + seawater	Adv. Mater. 2024, 36, 2408982.
OP-NiCo-LDH	500 mA cm^{-2}@500 h@330 mV	1 M KOH + seawater	Applied Catalysis B: Environmental. 2023, 332, 122749.
Ni_xCr_yO	500 mA cm^{-2}@100 h	1 M KOH + seawater	Angew. Chem. Int. Ed. 2023, 62, e202309854.
Nb-NiOOH-O_v	500 mA cm^{-2}@100 h	1 M KOH + seawater	ACS Nano. 2025, 19, 9070−9080.
Fe–NiSOH	500 mA cm^{-2}@1100 h@268 mV	1 M KOH + seawater	Energy Environ. Sci. 2022, 15, 4647–4658.
Co-$NiSe_2$	500 mA cm^{-2}@1500 h	1 M KOH + seawater	Applied Catalysis B: Environment and Energy. 2024, 344, 123658.
R-CoNiPS	500 mA cm^{-2}@200 h@420 mV	1 M KOH + seawater	Journal of Energy Chemistry. 2024, 94, 508–516.
CoNi-LDH/FeSe	500 mA cm^{-2}@500 h@338 mV	1 M KOH + seawater	Chemical Engineering Journal. 2024, 498, 155834.
$Ce_2(CO_3)_2O{\cdot}H_2O$@Fc	500mA cm^{-2}@300 h	1 M KOH + seawater	Chemical Engineering Journal. 2025, 507, 160375.
B-Co_2Fe LDH	500 mA cm^{-2}@100h	1 M KOH + seawater	Nano Energy 83 (2021) 105838.
((Ni,Fe)S_2@Ti_3C_2)	500 mA cm^{-2}@1000 h	1 M KOH + 0.5 M NaCl	Nature Communications. 2025, 16, 1319.
$(FeCoNiMnAl)_3O_4$	500 mA cm^{-2}@50 h	1 M KOH + seawater	Applied Catalysis B: Environment and Energy. 2024, 349, 123875.
NiFe LDH	400mA cm^{-2}@1000h	1 M NaOH +seawater +0.05 M Na_2SO_4	Angew. Chem. Int. Ed. 2021, 60, 22740 – 22744.
NiFe-LDH@Ag	400 mA cm^{-2}@2500 h	1 M KOH + seawater	Adv. Mater. 2024, 36, 2306062.
NiFeBa-LDH	400 mA cm^{-2}@10000 h	1 M NaOH + seawater + 0.05 M Na_2SO_4	Adv. Mater. 2024, 36, 2411302.

(Ni,Fe)O(OH)@NiCoSNAs	400、600 mA cm^{-2}@300 h	1 M KOH + seawater	Journal of Energy Chemistry. 2024, 91, 370–382.
S-(Fe)$Ni_2Mo_3O_8$	200 mA cm^{-2}@800 h@408 mV	1 M KOH + seawater	Chem Catalysis. 2024, 4, 101144.
Li-NiFe-LDH-g-C_3N_4	200 mA cm^{-2}@100 h	1 M KOH + seawater	Chemical Engineering Journal 2023, 473, 145293.
NiFe LDH-FLPs	200 mA cm^{-2}@250 h	1 M KOH + seawater	Angew. Chem. Int. Ed. 2025, 64, e202414721.
Mo-Ni_3S_2/VO_2	200 mA cm^{-2}@1500 h	1 M KOH + seawater	Applied Catalysis B: Environment and Energy. 2025, 365, 124925.
NiTe@FeOOH	100 mA cm^{-2}@100 h@280 mV	1 M KOH + seawater	Chemical Engineering Journal. 2023, 474, 145568.
Ni-BDC/NH_2-MIL-88B(Fe)	100 mA cm^{-2}@200 h@299 mV	1 M KOH + seawater	Adv. Funct. Mater. 2024, 34, 2314611.
NiFeCoP	100 mA cm^{-2}@100 h	1 M KOH + seawater	ACS Catal. 2024, 14, 18322−18332.
Mn–FeP_v	100 mA cm^{-2}@100 h	1 M KOH + seawater	Small. 2024, 20, 2308613.
MnFeCoNiPS_3	100 mA cm^{-2}@1200 h@313 mV	1 M KOH + seawater	Adv. Funct. Mater. 2025, 2417211.
LiFePO4	100 mA cm^{-2}@600 h	1 M KOH + seawater	Angew. Chem. Int. Ed. 2024, 63, e202410396.
$(CoMo)_{0.85}$Se@FeOOH	50 mA cm^{-2}@140 h	1 M KOH + 0.5 M NaCl	ACS Catal. 2023, 13, 15360−15374.
Ni3Fe-LDHs@CoP_x	10 mA cm^{-2}@350 h@370 mV	1 M KOH + seawater	Chemical Engineering Journal. 2023, 460 141413.
NiFe@DG	10 mA cm^{-2}@2000 h@218 mV	1 M KOH + seawater	ACS Nano. 2023, 17, 18372−18381.
Ni_3S_2@FeOOH/NF	1000 mA cm^{-2}@1400 h 2000 mA cm^{-2}@500 h	1 M KOH + seawater	This work

References

[1] S. Vijay, W. Ju, S. Brückner, S.-C. Tsang, P. Strasser, K. Chan, Nat. Catal. 2021, 4 1024−1031.

[2] J. Santatiwongchai, K. Faungnawakij, P. Hirunsit, ACS Catal. 2021, 11, 9688−9701.

[3] N. Yang, L. Peng, L. Li, J. Li, Q. Liao, M. Shao, Z. Wei, Chem. Sci. 2021, 12, 12476−12484.

[4] L. Zhang, J. Liang, X. He, Q. Yang, Y. Luo, D. Zheng, S. Sun, J. Zhang, H. Yan, B. Ying, X. Guo, X. Sun, Inorg. Chem. Front. 2023, 10, 2100−2106.

[5] J. G. Vos, M. T. M. Koper, J. Electroanal. Chem. 2018, 819, 260–268.